The Rational of Catalytic Activity of Herpes Simplex Virus Thymidine Kinase

A COMBINED BIOCHEMICAL AND QUANTUM CHEMICAL STUDY*

Marialore Sulpizi‡§, Pierre Schelling¶‖, Gerd Folkers¶, Paolo Carloni‡§‡‡, and Leonardo Scapozza¶§§**

*From the ‡Scuola Internazionale Superiore di Studi Aranzati, International School for Advanced Studies, via Beirut 2-4, 34013 Trieste, Italy, the §Istituto Nazionale di Fisica della Materia, 34014 Trieste Italy, the ¶Department of Applied BioSciences,, Institute of Pharmaceutical Sciences, Swiss Federal Institute of Technology, Winterthurerstrasse 190, CH-8057 Zürich, Switzerland, and the **International Centre for Genetic Engineering and Biotechnology, AREA Science Park, Padriciano 99, 34012 Trieste, Italy*

Most antiherpes therapies exploit the large substrate acceptance of herpes simplex virus type 1 thymidine kinase (TK_{HSV1}) relative to the human isoenzyme. The enzyme selectively phosphorylates nucleoside analogs that can either inhibit viral DNA polymerase or cause toxic effects when incorporated into viral DNA. To relate structural properties of TK_{HSV1} ligands to their chemical reactivity we have carried out *ab initio* quantum chemistry calculations within the density functional theory framework in combination with biochemical studies. Calculations have focused on a set of ligands carrying a representative set of the large spectrum of sugar-mimicking moieties and for which structural information of the TK_{HSV1}-ligand complex is available. The k_{cat} values of these ligands have been measured under the same experimental conditions using an UV spectrophotometric assay. The calculations point to the crucial role of electric dipole moment of ligands and its interaction with the negatively charged residue Glu^{225}. A striking correlation is found between the energetics associated with this interaction and the k_{cat} values measured under homogeneous conditions. This finding uncovers a fundamental aspect of the mechanism governing substrate diversity and catalytic turnover and thus represents a significant step toward the rational design of novel and powerful prodrugs for antiviral and TK_{HSV1}-linked suicide gene therapies.

The thymidine kinase from herpes simplex virus type 1 (TK_{HSV1})[1] salvages thymine into the metabolism of the virus by converting it to thymidine monophosphate (1). In contrast to the human isoenzyme, TK_{HSV1} acts as phosphorylating agent toward a large variety of nucleoside analogs such as (North)-methanocarba-thymidine (n-MCT), aciclovir (ACV), ganciclovir (GCV), and penciclovir (PCV). These analogs exhibit chemical diversity for the nucleobase as well as for the sugar-like chain moiety (2, 3) (Fig. 1). Substrate diversity of TK_{HSV1} provides the molecular basis for effective and selective treatment of virus infections. It is also exploited for gene therapy approaches involving TK_{HSV1} as suicide gene by anticancer intervention (4) or the control of graft *versus* host disease by allogeneic bone marrow transplantation (5).

The recent determination of the x-ray structure of a large spectrum of ligand-enzyme complexes (6–11) has opened a new avenue for the understanding structure-function relationships as well as of the functional role of amino acids involved in binding. It has emerged that the enzyme accommodates the nucleobase and sugar-like chain moieties in two different pockets (P1 and P2 in Fig. 2), interacting with the ligand by a specific and extensive H-bond network.

In the pocket P1, the nucleobase moiety (either a thymine or a guanine ring) is stabilized by direct H bonds with the highly conserved Gln^{125} and with Arg^{176} by means of two ordered water molecules. The pyrimidine ring is further fixed by a peculiar interaction with Tyr^{172} and Met^{128} (11) in a sandwich-like orientation (Refs. 12 and 13 and Fig. 2).

In P2, the sugar-like chains interact with the protein via its hydroxyl groups. The 3′-OH (and its mimics) forms specific H bonds with Tyr^{101} and/or Glu^{225} (Figs. 2 and 3), whereas 5′-OH forms a direct H bond or water-mediated interactions with Arg^{163}, Glu^{83}, and Arg^{222} (Figs. 2 and 3). In contrast, the polar C-1′–O-4′–C-4′ function belonging to dT and the correspondent ether groups of ACV and GCV interact neither with polar or charged groups of the protein nor with the solvent; instead, they point toward a hydrophobic region made up of the Trp^{88}, Ile^{97}, and Met^{128} side chains (Fig. 4).

Key aspects of nucleoside binding have been recently elucidated by theoretical (12) and experimental (6–11) approaches. In contrast, fundamental questions regarding the nature of the interactions between the ribose-like moiety and the enzyme are still open. First, it is rather intriguing that the accessibility of the 5′-OH mimic to the ATP cofactor is roughly the same
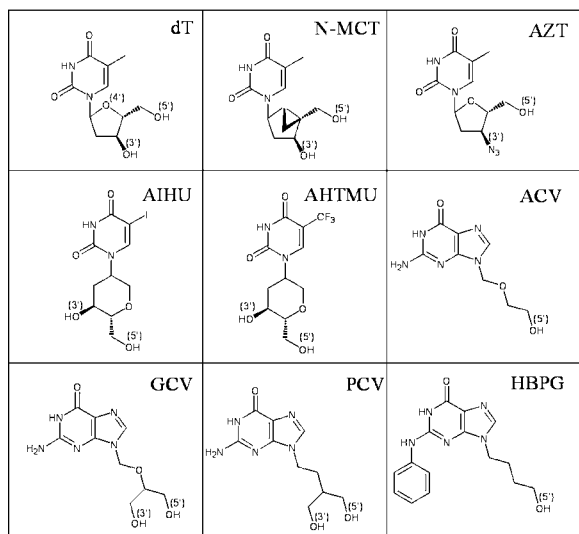
FIG. 1. **Chemical formulas of selected (fraudulent) substrates and inhibitors of TK$_{HSV1}$.** dT is the natural substrate; n-MCT, ACV, PCV, GCV, AHIU, AHTMU, and AZT are prodrugs; and HBPG is an inhibitor. The 5′-OH and 3′-OH groups belonging to dT and their mimics are labeled.
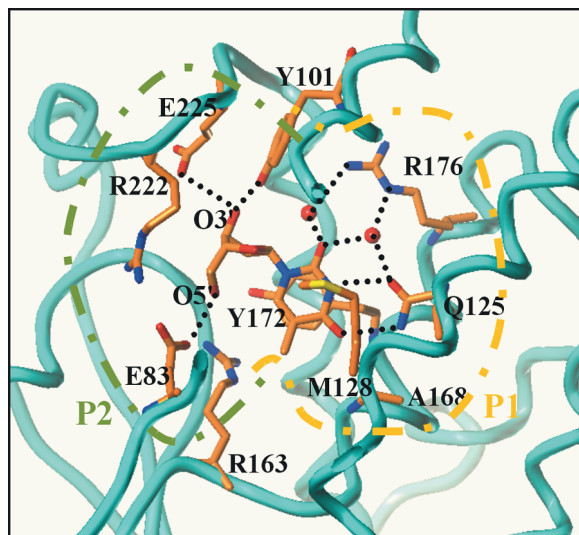

FIG. 3. **Quantum mechanical model for dT-HSV-1 TK complex.** The water molecules are represented as *red spheres*, and the hydrogen bonds are shown as *dotted lines*.

FIG. 2. **X-ray structure for the thymidine kinase active site (11).** *P1* and *P2* are the active site portions that accommodate the nucleobase and the sugar-like moiety, respectively. The water molecules are shown as *red spheres*, and the hydrogen bonds are depicted as *dotted lines*. dT and the amino acids are displayed as *capped sticks* and are color coded. *Orange*, carbon; *red*, oxygen; *blue*, nitrogen; yellow, sulfur. The rest of the protein is shown as a ribbon model. The picture was generated with the program SYBYL (Tripos Inc., St. Louis, MO).

FIG. 4. *a*, dT-TK$_{HSV1}$ complex. Orientation of O-4′ in its hydrophobic pocket. *b* and *c*, sugar (*b*) and methylene derivative (*c*) electric dipoles.

(Fig. 5), yet the HBPG molecule, which shares the same binding mode as the structurally related prodrug aciclovir (6), *inhibits* the enzyme. Furthermore, it is not known why the k_{cat} values of prodrugs are much smaller than that of the natural substrate (see Table I), although the protein-sugar mimicking H bonding interactions is very similar (Fig. 5). Finally, as discussed above, it is rather surprising that the environment accommodating the inner sugar ring C-1′–O-4′–C-4′ group of the natural substrate is totally hydrophobic (Fig. 4).

In this paper we address these fundamental issues by performing a combined quantum chemical and biochemical investigation of sugar and sugar-like moieties of substrates and inhibitors of TK$_{HSV1}$. The theoretical methodology is based on gradient-corrected density functional theory. This approach allows an accurate description of electrostatic and hydrogen-
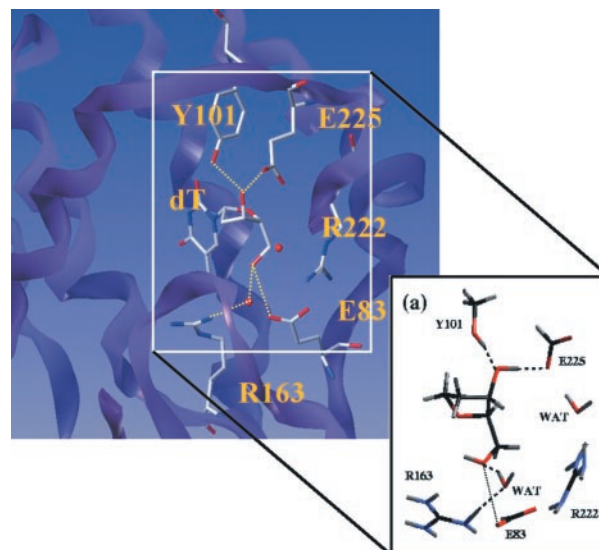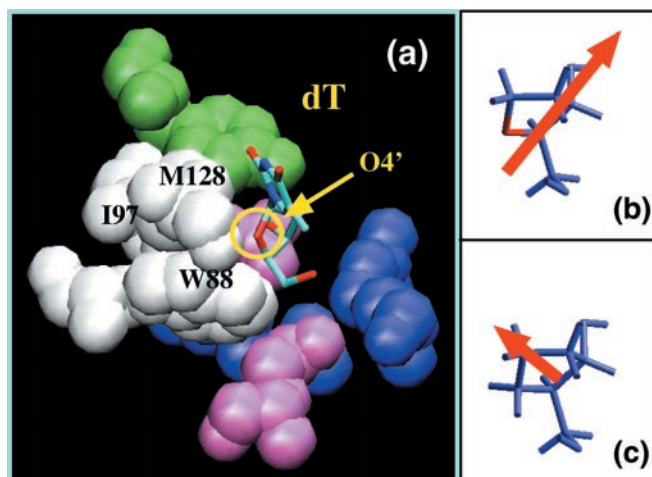
bonded complexes (12, 14–17), such as those investigated here. The biochemical study involves the measurement of the catalytic constant (k_{cat}) of dT and prodrugs using a modified UV spectrophotometric assay based on pyruvate kinase and lactate dehydrogenase (3). This assay does not require the use of radioactively labeled compounds. This provided a set of homogeneous data, which is necessary for a proper comparison with the quantum chemical calculation. As we will show, the interaction between the *electric dipole* of the sugar mimicking moiety and the *negative charge* of the conserved residue Glu[225] correlates with the k_{cat} measurements and thus is a critical factor for the phosphorylation reaction.

EXPERIMENTAL PROCEDURES
Biochemical Essays

Materials—PreScission protease was purchased from Amersham Pharmacia Biotech. AZT and reagents for enzyme assays were obtained from Sigma. Strain BL21 (Amersham Pharmacia Biotech) served as the expression host. n-MCT and PCV were kindly provided by Dr. Marquez (National Institutes of Health, Bethesda, MD) and Dr. Johannsen (Forschungszentrum Rossendorf Institute of Bioinorganic and Radiopharmaceutical Chemistry Research Center, Rossendorf, Germany), respectively. 5-Trifluoromethyl anhydrohexitoluridine (AHTMU), AHIU analogs, and HBPG were gifts of Dr. De Clercq (Rega Institute Katholike Universiteit Leuven, Belgium) and Dr. Wright (University of
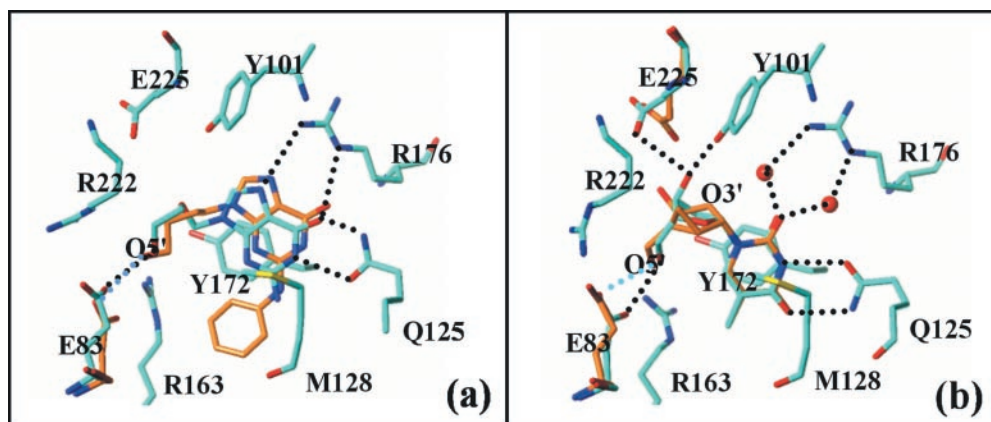
An ab Initio and Biochemical Investigation on HSV-1 TK

FIG. 5. **Active site superposition of representative ligands of the guanine (*a*) and thymine (*b*) series.** *a*, the structure of the substrate ACV in complex with TK[HSV1] (6) is superimposed with that of the inhibitor HBPG (6). It clearly shows that the inhibitor in *orange* shares the same binding mode as the substrate ACV in *cyan*. In both cases the 5′-OH mimicking group are at a hydrogen bond distance from Glu[83] and points toward the phosphate moiety of ATP. For the sake of clarity the superimposed GCV and PCV sharing the same binding mode of ACV (6) are not shown. The H bond network of ACV is shown as *dotted lines* as a representative for all guanine derivatives. *b*, the structure of the natural substrate dT (*cyan*) ligated to TK[HSV1] (8) is superimposed with that of TK[HSV1]:n-MCT (9) (*orange*). Both natural substrate and the prodrug share the same binding mode with the 5′-OH mimicking group pointing toward Glu[83]. AHTMU and AZT (6) have the same binding mode, and they are not shown for clarity. The H bond network of dT is shown as *dotted lines* as a representative for all thymine derivatives in respect to the base and the 5′-OH position. In contrast, the interaction of the 3′-OH mimicking group with Glu[225] and Tyr[101] varies depending on the ligand. All residues of the TK[HSV1]:HBPG and TK[HSV1]:n-MCT that take the same conformation as in TK[HSV1]:ACV and TK[HSV1]:dT, respectively, were omitted for the sake of clarity.

Massachussets, Worcester, MA), respectively. ACV and GCV were purchased by Glaxo-Wellcome and Roche, respectively. dT was obtained from Fluka.

Expression and Purification of TK[HSV1]—TK[HSV1] was expressed as gluthathione *S*-transferase fusion protein in competent *Escherichia coli* BL21 using the vector pGEX-6P-2-TK (9). The protein was purified by gluthathione-affinity chromatography followed by on-column PreScission protease cleavage using a previously described protocol (9). Purification was monitored by SDS-polyacrylamide gel electrophoresis and led to a >90% pure TK[HSV1], which was directly used for k_{cat} determination. Total protein concentration was measured using the Bio-Rad protein assay.

Spectrophotometric Assay for k_{cat} Determination—An UV spectrophotometric test based on a lactate dehydrogenase-pyruvate kinase coupled assay (3) was employed to monitor ADP formation during substrate phosphorylation. The concentrations of ATP and the ligands were 5 and 1 mM, respectively. These concentrations are at least five time higher than the binding affinities of the studied compounds allowing the measurement of V_{max} and thus of k_{cat} ($k_{cat} = V_{max}/[E]$). The change in absorbance at 340 nm was recorded over time and correlates with the k_{cat} of the analyzed substrates for which values were known from the literature and allows the determination of k_{cat} for compounds that are not available in radiolabeled form (see Table I).

Quantum Chemical Calculations

Our structural models for quantum chemical calculation on the sugar moiety of dT-, ACV-, GCV-, PCV-, n-MCT-, and HBPG-TK[HSV1] were constructed from the correspondent crystal structures (Protein Data Bank codes 1kim, 2ki5, 1ki2, 1ki3, 1e2k, and 1qhi) (6, 8, 9). The resolution of the structures ranges from 1.7 to 2.4 Å.

The structure of AHTMU-TK[HSV1] has not been solved yet, whereas the structure of the complex AHIU-TK[HSV1] is known (Protein Data Bank code 1ki6) (8). AHIU is chemically and structurally extremely similar to AHTMU (Fig. 1); the two analogs differ only for the group at position 5 of the nucleobase ring (a iodine in AHIU and a CF_3 in AHTMU). All available structural data show that this substitution does not affect the binding orientation of the sugar mimicking moiety (8). The initial configuration of AHTMU is therefore built from this x-ray structure.

The x-ray structure of the AZT-TK[HSV1] complex is not available, and therefore one has to resort to theoretical structural models. Here we used molecular dynamics-based models reported earlier (18).

The complexes included the sugar-like moieties of the ligands and part of side chains of all of the groups directly interacting with it or forming water-mediated hydrogen bonds (Tyr[101], Arg[163], Glu[83], Glu[225], and Arg[222]). Trp[88], Ile[97], and Met[128] side chains were not included because (i) they would have dramatically increased the size of our model

TABLE I
Values of catalytic activity (k_{cat}) of compounds listed in Fig. 1

The values are the results of at least five independent experiments. ND, not determined.

Compound	k_{cat}[a]	k_{cat} (from literature)	k_{cat} as rate percentage of dT[b]
	s^{-1}	s^{-1}	%
dT	0.348 ± 0.004	0.35[c]–0.45[d]	100
ACV	0.115 ± 0.025	0.015[d]–0.101[e]	27
GCV	0.100 ± 0.017	0.102[d]	ND
PCV	0.045 ± 0.019	ND	9
AHTMU	0.210 ± 0.048	ND	ND
n-MCT	0.178 ± 0.010	ND	ND
AZT	0.044 ± 0.018	0.056[c]	ND
HBPG	0	0[f]	ND

[a] This work.
[b] The rate percentages were determined using the substrates at 250 μM (34).
[c] Ref. 32.
[d] Ref. 31.
[e] Ref. 33.
[f] HBPG is an inhibitor.

complexes, (ii) they do not contribute significantly to the electrostatic interactions (the focus of the present work) because they form only weak hydrophobic contacts with the sugar, and (iii) the position of these groups is essentially the same in all of the complexes investigated here (6, 8, 9) and therefore their contribution is expected to be rather constant. Hydrogen atoms were added assuming standard bond lengths and bond angles. In Fig. 3 the quantum mechanical model for dT, the natural substrate, is shown in detail. The overall charge of our complexes is 0.

The calculations were performed within the framework of density functional theory (19) in its Kohn and Sham (20) formulation. In this approach the use of gradient corrections is crucial for correctly describe hydrogen bond interactions. Here we used the prescription of Becke and Lee (41, 43) because it has been shown to provide an accurate description of water and hydrogen bonding in biological systems (14, 15, 21, 22). The basis set consisted of a plane wave basis set up to a cut-off of 70 Rydberg, the interactions between valence electrons and ionic cores being described by pseudopotentials of the Martins-Troullier type (23). Only the Γ point was used. The dT-TK complex was inserted in orthorombic box with edges $14 \times 15 \times 16$ Å^3. Similar box sizes were used for all of the other complexes. In all circumstances the separation between periodic images was at least 6 Å. However, the Coulombic interaction between images was screened using the approach of Barnett and Landman (24). Geometry optimization was performed using the direct inversion iterative subspace (25). Cα

TABLE II

Structure, catalytic activity, and electrostatic interactions in ligand-TK$_{HSV1}$ complexes

RMS deviations between x-ray and optimized structure are reported in Å; dipole moments are in Debye. Glu^{225} and Arg^{163} sugar-like chain interactions are reported in arbitrary units.

Compound	RMS	k_{cat}	Dipole (D)	Dipole-GLU225 energy	Dipole-Arg^{163} energy
	Å	s^{-1}			
dT	0.19	0.348 ± 0.004	1.74	−4.5	−3.1
ACV	0.26	0.115 ± 0.025	1.96	−1.5	−2.2
GCV	0.27	0.100 ± 0.017	1.74	−1.3	−3.4
PCV	0.35	0.045 ± 0.019	1.31	0.0	−0.4
AHTMU	0.26	0.210 ± 0.048	0.40	−1.0	−0.4
n-MCT	0.17	0.178 ± 0.010	2.83	−1.0	−4.9
AZT	0.24	0.044 ± 0.018	3.26	4.9	4.7
HBPG	0.15	0	1.74	0.8	−2.0

TABLE III

dT/TK optimized structure: bond lengths, angles, and torsional angles of the sugar moiety

Deviations from the crystallographic structure are shown in parentheses.

Bond length		Angle		Torsional angle	
	Å		°		°
O-5–C-5	1.48 (0.01)	O-5—C-5—C-4	110 (−2)	O-5—C-4—C-3—C-2	56 (6)
C-5–C-4	1.52 (0.01)	C-5—C-4—C-3	116 (5)	C-5—C-4—C-3—C-2	−105 (−14)
C-4–C-3	1.57 (0.06)	C-4—C-3—C-2	103 (0)	C-4—C-3—C-2—C-1	−36 (10)
O-3–C-3	1.44 (0.04)	O-3—C-3—C-4	110 (6)	C-3—C-2—C-1—O-4	46 (9)
C-3–C-2	1.54 (0.02)	C-3—C-2—C-1	100 (−4)	O-3—C-3—C-2—C-1	81 (17)
C-2–C-1	1.52 (0.04)	C-2—C-1—O-4	104 (8)	C-2—C-1—O-4—C-3	−39 (−20)
C-1–O-4	1.47 (0.01)	C-1—O-4—C-4	106 (−13)	C-1—O-4—C-4—C-3	15 (23)
O-4–C-4	1.48 (0.05)	O-4—C-4—C-3	106 (8)	O-4—C-4—C-3—C-2	14 (−17)

FIG. 6. **Electric dipoles of HSV-1 TK sugar-like chains.** *a*, dT; *b*, n-MCT; *c*, AHTMU; *d*, AZT; *e*, ACV; *f*, HBPG; *g*, GCV; *h*, PCV.
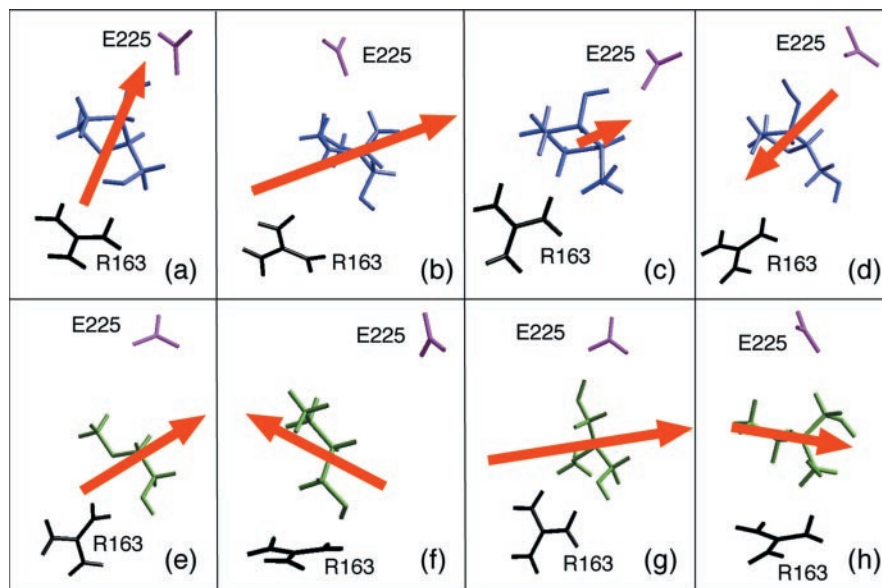
atoms were constrained to crystallographic positions to take into account the reduced mobility of residues caused by protein environment. A similar procedure has been reported elsewhere (14).

The electronic structure was described with the geometrical analysis of centers of maximally localized Wannier functions (WFC) (26–28). This analysis is useful for investigating the polarity of chemical bonds, because WFC shifts are related quantitatively to the differences $\Delta\chi$ of Pauling electronegativities (29) with respect to the noninteracting compounds (22); an increase of $\Delta\chi$ corresponds to an increase of polarization of the electronic density in the X-Y bond toward the most electronegative atom X. The effects of the protein electric field were estimated through a comparison of Wannier center shifts for the system in vacuum or in the presence of a protein electric field. The procedure was identical to that of Piana and Carloni (14). Interaction energies between the substrate and the active site are calculated within the central dipole approximation (30) where the dipole is the result of the quantum calculation. Interaction energy was calculated as $E_{charge-dipole} = (\xi \, \mu \cdot R)/(4\pi\epsilon_0 R^3)$, where R is the distance vector between the centers of charges of the sugar moiety and the residue of charge ξ and μ is the dipole moment for the sugar moiety.

Even if the expansion is limited to large distances between two interacting groups, this model can provide quantitative results for a comparison between systems that have similar geometries. We have reported the energetics in arbitrary units.

RESULTS

Catalytic Activity of TK$_{HSV1}$

The catalytic activity of TK$_{HSV1}$ with the compounds listed in Fig. 1 was measured under the same conditions. Table I shows that the measured k_{cat} of dT agrees with those reported in literature (31, 32). Also the k_{cat} of ACV corresponds to that measured in two independent laboratories (33, 34). In the literature a value of 0.015 s^{-1} is also reported for ACV (31), but, considering the newly reported values, this seems to be an outlier. The k_{cat} values of GCV and PCV are also congruent
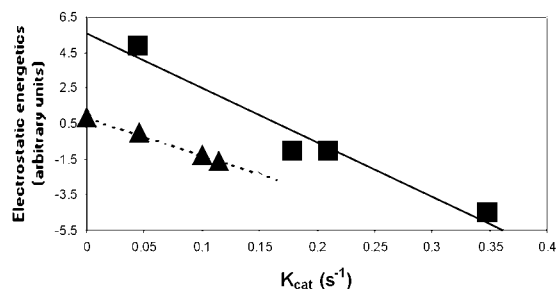
FIG. 7. **Correlation between k_{cat} and the sugar-moiety-dipole-Glu^{225} electrostatic energy (electrostatic energetics).** Thymine and guanine derivatives are displayed as *squares* and *triangles*, respectively. Linear fits are also plotted (R^2 values of thymine and guanine are 0.954 and 0.994, respectively).

with the literature values (31, 34). The same agreement has been found for AZT whose k_{cat} value is 0.044 s^{-1}. The k_{cat} values of the new compounds AHTMU and n-MCT have been reported here for the first time.

Quantum Chemistry Calculations

Overall, the geometry of the complexes are in very good agreement with the experimental structural data as shown by the low root mean squared deviation values between experimental and optimized structures (Table II). In particular Table III shows that the structural parameters of the geometry optimized systems are in good agreement with experimental data. Thus our first principle approach appears to reproduce very reliably the structural properties of the adducts. Geometry optimization permits also us to establish the H bond network between the substrate and the enzyme that is crucial in determining the electrostatic properties of the adducts and that is only indirectly deducible from the crystal structure where hydrogen atoms are missing.

Enzyme-Sugar Interactions—One of the most important physical properties of polar molecules such as ribose and its analogs is given by their electric dipole moment. Fig. 6 offers a visual representation of the calculated dipoles projected to the geometry-optimized structure. The dipole of the sugar moiety of the natural substrate aligns strikingly to the negatively charged Glu^{225} group. Interestingly, the dipoles of most of the prodrugs investigated here also point to these residues. The calculated stabilization energy resulting from the electrostatic interaction is the maximum for the natural substrate (Table III). The dipoles of AZT and the inhibitor HBPG do not point toward the negative residue and as a consequence the interaction energy is repulsive.

In an attempt at correlating electrostatic interactions with kinetics data, we first subdivide the compounds into two major classes. The first class includes the compounds bearing a thymine or a thymine-substituted base (namely dT, AHTMU, n-MCT, and AZT); the second class includes the compounds bearing guanine (ACV, HBPG, GCV, and PCV).

The subdivision is necessary as the computational model did not include the base and consequently the electrostatic calculations do not consider the contributions of the nucleobases (12), whose dipole moments are different but additive.[2] In Fig. 7, the correlation between the interaction energy dipole-Glu^{225} and the catalytic constant of the studied ligands appears clearly. The slope of the linear fit depends on the type of sugar mimicking moiety of the ligand. The additivity of the sugar-like

---

[2] The contribution of the nucleobase of the nucleotides to the dipole interaction was additive, even if different for thymine and guanine. Because the chemical bond between the nucleobase and the sugar moiety is nonpolar, we have verified the additivity of the nucleobase and sugar moiety dipoles.
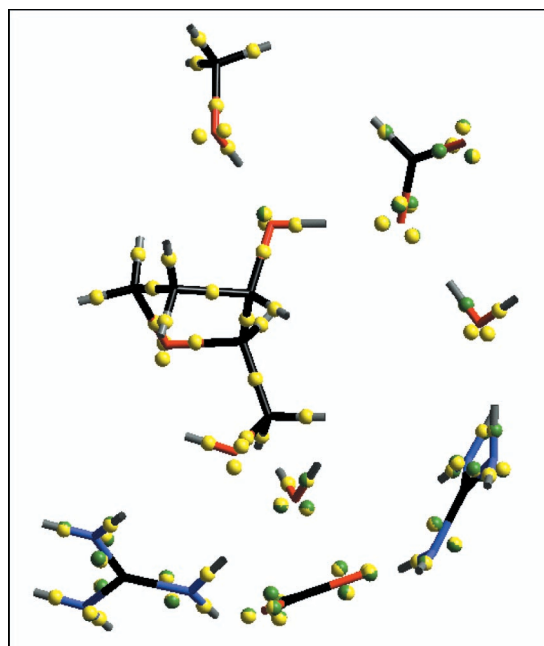

FIG. 8. **Electronic structure of the model for the dT-HSV-1 TK active site.** The Wannier centers (26–28) in the presence and the absence of the protein electrostatic potential are represented as *yellow* and *green spheres*, respectively.

chains and the nucleobase dipoles is confirmed by a rigid shift between the linear fit for the guanine and thymine derivatives (Fig. 7).

The Roles of Arg^{222}, Arg^{163}, and Glu^{83} Interacting Groups—Although there is no direct correlation between the k_{cat} and the Arg^{163}-dipole interaction, the calculated interaction between Arg^{163} and the sugar is important, consistent with previously published mutagenesis experiments (35). From the crystallographic and mutagenesis studies, Arg^{222} and Glu^{83} are essential elements of the kinase machinery; Arg^{222} forms the anion hole with Arg^{220} to make the phosphate atom more electrophilic, and Glu^{83} behaves as base on the O-5$'$ atom, causing an increase in nucleophily. Thus it is not surprising that the Arg^{222}- and Glu^{83}-dipole interactions appear not to have any direct correlation with k_{cat} (data not shown), because their influence is based on a totally different mechanisms.

Sugar-TK$_{HSV1}$ Hydrophobic Interactions—Our calculations have pointed to the crucial role of the electric dipole moment of the sugar moieties. We now address the following question. In the natural substrate, is the polar C-1$'$–O-4$'$–C-4$'$ (which faces a hydrophobic pocket; Fig. 4a) important for the correct orientation of the dipole? To answer this question, we calculate the change of electric dipole associated with replacement of O-4$'$ with the CH$_2$ apolar group (Fig. 4b). Our calculations show that the resulting dipole is both smaller and different in orientation relative to the sugar moiety (Fig. 4, b and c). We conclude that the polar function is essential for a correct alignment of the dipole to the Glu^{225} charge.

Protein Environment Effects—The field of the protein may be very important for the chemistry of the active site of this and other enzymes (36). Here we estimate the effect of the protein frame by comparing the electronic structure of the complexes in a vacuum with those in the presence of the protein. A convenient representation of the electronic structure is given by the Wannier functions, whose centers (WFC) represent chemical concepts such as lone pairs and chemical bonds. Fig. 8 shows that there is no appreciable displacement of the WFC, so that it is possible to conclude that the main contribution to the

interaction is included in the model we have chosen for quantum mechanics calculations.

DISCUSSION

Deciphering the binding mode of prodrugs to the enzyme and their catalytic turnover may help to rationally design more and potent prodrugs for antiviral therapy to overcome the problems of resistance or to be used in enzyme-prodrug gene therapy as well as improve variants of TK_{HSV1} for gene therapeutic approaches (37).

The mechanisms ruling binding affinities toward TK_{HSV1} have been previously presented (8, 9, 12, 38). However, the intriguing question posed by the recently published crystal structure of the inhibitor HBPG (6, 9) as to what is the structural basis for the different properties between inhibitor and substrate sharing the same binding mode remained open. This issue prompted us to perform a combined biochemical and quantum chemical study. Two key parameters have been considered: on the one hand binding affinity and on the other hand catalytic turnover.

Because not all k_{cat} values were available and some conflicting kinetics results had been reported in the literature (Table I), the catalytic activity of TK_{HSV1} toward all ligands has been measured under the same experimental conditions. In this way, a homogeneous set of measured k_{cat} values have been obtained and compared with the calculations.

The calculated sugar dipole points to Glu^{225}, and the resulting stabilization energy correlates strikingly with the catalytic activity (Fig. 7). These results are consistent with a previously published study on E225L TK_{HSV1}. Indeed this mutant exhibits a loss in binding affinity proportional to the loss of one hydrogen bond and, more interestingly, a dramatic drop in catalytic activity (32).

Glu^{225} contributes to the binding affinity of the prodrug by H bond interactions with the 3′-OH group (7–11). Our calculations point to its important role in catalysis derived from its interaction with the dipole. In contrast no correlation have been found between the calculated terms and binding affinity expressed as K_i or K_m. This type of calculations are very straightforward and can be extended in the future to new compounds.

Because the dominating component of the sugar-like chain-protein interactions and correlations is electrostatic, one might think about using molecular mechanics calculation for performing similar studies (42). We performed such a calculation on some of the complexes, and indeed the results are very promising (data not shown). These calculations, however, required the development of the force field parameters of the prodrugs, which in turn required quantum chemical calculation. Therefore, the calculation effort using force field methodologies is not reduced compared with the quantum chemical calculation. On the other hand, the latter, being a parameter-free approach, allows an automatic procedure studying prodrug-enzyme interactions.

Our study also provides a rationale for the presence of the polar group in the hydrophobic pocket of the enzyme (Fig. 4). Indeed, replacement of the O-4′ with a CH_2 group ether provides a dramatic reduction and a change of orientation of the dipole (Fig. 4, *b* and *c*), which in turn could decrease the stabilizing dipole-Glu^{225} interactions.

In conclusion we indicated a substrate-enzyme molecular interaction that has been shown to be relevant to catalysis. We have shown a nice correlation between the dipole-charge (substrate-Glu^{225}) interaction and the catalytic activity, which suggests this electrostatic contribution as a stabilizing mechanism for catalysis. Up to now all prodrugs have been the results of nucleobase or sugar moiety substitution with the only rational guide of mimicking the sugar moiety assuming the importance of elements such as the O-4′ but not knowing the exact role. With our work we suggest a guide element in the rational design of novel nucleosides analogs having an increased phosphorylating activity.

REFERENCES

1. Chen, M. S., and Prusoff, W. H. (1978) *J. Biol. Chem.* **253,** 1325–1327
2. Elion, G. B., Furman, P. A., Fyfe, J. A., de Miranda, P., Beauchamp, L., and Schaeffer, H. J. (1977) *Proc. Natl. Acad. Sci. U. S. A.* **74,** 5716–5720
3. Keller, P. M., Fyfe, J. A., Beauchamp, L., Lubbers, C. M., Furman, P. A., Schaeffer, H. J., and Elion, G. B. (1981) *Biochem. Pharmacol.* **30,** 3071–3077
4. Culver, K. W., Ram, Z., Wallbridge, S., Ishii, H., Oldfield, E. H., and Blaese, R. M. (1992) *Science* **256,** 1550–1552
5. Bonini, C., Ferrari, G., Verzeletti, S., Servida, P., Zappone, E., Ruggieri, L., Ponzoni, M., Rossini, S., Mavilio, F., Traversari, C., and Bordignon, C. (1997) *Science* **276,** 1719–1724
6. Bennett, M. S., Wien, F., Champness, J. N., Batuwangala, T., Rutherford, T., Summers, W. C., Sun, H., Wright, G., and Sanderson, M. R. (1999) *FEBS Lett.* **443,** 121–125
7. Brown, D. G., Visse, R., Sandhu, G., Davies, A., Rizkallah, P. J., Melitz, C., Summers, W. C., and Sanderson, M. R. (1995) *Nat. Struct. Biol.* **2,** 876–881
8. Champness, J. N., Bennett, M. S., Wien, F., Visse, R., Summers, W. C., Herdewijn, P., de Clerq, E., Ostrowski, T., Jarvest, R. L., and Sanderson, M. R. (1998) *Proteins* **32,** 350–361
9. Prota, A., Vogt, J., Perozzo, R., Pilger, B. D., Wurth, C., Marquez, V., Russ, P., Schulz, G., Folkers, G., and Scapozza, L. (2000) *Biochemistry* **39,** 9597–9603
10. Wild, K., Bohner, T., Aubry, A., Folkers, G., and Schulz, G. E. (1995) *FEBS Lett.* **368,** 289–292
11. Wild, K., Bohner, T., Folkers, G., and Schulz, G. E. (1997) *Protein Sci.* **6,** 2097–2106
12. Alber, F., Kuonen, O., Scapozza, L., Folkers, G., and Carloni, P. (1998) *Proteins* **31,** 453–459
13. Kussmann-Gerber, S., Kuonen, O., Folkers, G., Pilger, B. D., and Scapozza, L. (1998) *Eur. J. Biochem.* **255,** 472–481
14. Piana, S., and Carloni, P. (2000) *Proteins* **39,** 26–36
15. De Santis, L., and Carloni, P. (1999) *Proteins* **37,** 611–618
16. Roethlisberger, U., Carloni, P., Doklo, K., and Parrinello, M. (2000) *J. Biol. Inorg. Chem.*
17. Roethlisberger, U., and Carloni, P. (1999) *Int. J. Quantum Chem.* **73,** 209–218
18. Christians, F. C., Scapozza, L., Crameri, A., Folkers, G., and Stemmer, W. P. (1999) *Nat. Biotechnol.* **17,** 259–264
19. Hohenberg, P., and Kohn, W. (1964) *Phys. Rev. B* **136,** 864–871
20. Kohn, W., and Sham, L. J. (1965) *Phys. Rev. A* **140,** 1133–1138
21. Molteni, C., Frank, I., and Parrinello, M. (1999) *J. Am. Chem. Soc.* **121,** 12177–12183
22. Alber, F., Folkers, G., and Carloni, P. (1999) *J. Phys. Chem. B* **103,** 6121–6126
23. Troullier, N., and Martins, J. L. (1991) *Phys. Rev. B* **43,** 1943–2006
24. Barnett, R. N., and Landman, U. (1993) *Phys. Rev. B* **48,** 2081–2097
25. Pulay, P. (1980) *Chem. Phys. Lett.* **73,** 393–398
26. Silvestrelli, P. L., Marzari, N., Vanderbilt, D., and Parrinello, M. (1998) *Solid State Commun.* **107,** 7–11
27. Silvestrelli, P. L., and Parrinello, M. (1999) *Phys. Rev. Lett.* **82,** 3308–3311
28. Marzari, N., and Vanderbilt, D. (1997) *Phys. Rev. B* **56,** 12847–12865
29. Hehre, W. J., Radom, L., Schleyer, P. V. R., and Polple, J. (1986) *Ab initio Molecular Orbital Theory*, p. 140, John Wiley & Sons, Inc., New York
30. Leach, A. (1996) *Molecular Modelling, Principles and Applications*, Addison Wesley Longman, Essex, UK
31. Kokoris, M. S., Sabo, P., Adman, E. T., and Black, M. E. (1999) *Gene Ther.* **6,** 1415–1426
32. Pilger, B. D., Perozzo, R., Alber, F., Wurth, C., Folkers, G., and Scapozza, L. (1999) *J. Biol. Chem.* **274,** 31967–31973
33. Kussmann-Gerber, S., Wurth, C., Scapozza, L., Pilger, B. D., Pliska, V., and Folkers, G. (1999) *Nucleosides Nucleotides* **18,** 311–330
34. VereHodge, R. A. (1993) *Antiviral Chem. Chemother.* **4,** 67–84
35. Black, M. E., and Loeb, L. A. (1993) *Biochemistry* **32,** 11618–11626
36. Warshel, A. (1998) *J. Biol. Chem.* **273,** 27035–27038
37. Encell, L. P., Landis, D. M., and Loeb, L. A. (1999) *Nat. Biotechnol.* **17,** 143–147
38. Perozzo, R., Jelesarov, I., Bosshard, H. R., Folkers, G., and Scapozza, L. (2000) *J. Biol. Chem.* **275,** 16139–16145
39. Hutter, J., Ballone, P., Bernasconi, N., Focher, P., Fois, E., Godecker, S., Parrinello, M., and Tuckerman, M. (1996) *CPMD*, version 3.0h, MPI fur Festkorperforschung and IBM Zurich Research Laboratory, Zurich, Switzerland
40. Xu, H., Maga, G., Focher, F., Smith, E. R., Spadari, S., Gambino, J., and Wright, G. E. (1995) *J. Med. Chem.* **38,** 49–57
41. Becke, A. De. (1988) *Physiol. Rev. A* **38,** 3098–3100
42. Case, D. A., Pearlman, D. A., Caldwell, J. W., Cheatham, T. E., III, Ross, W. S., Simmerling, C. L., Darden, T. A., Merz, K. M., Stanton, R. V., Cheng, A. L., Vincent, J. J., Crowley, M. F., Ferguson, D. M., Radmer, R. J., Singh, U. C., Weiner, P. K., and Kolman, P. A. (1997) AMBER 5.0, University of California, San Francisco, CA
43. Lee, C., Yang, W., and Parr, R. G. (1988) *Physiol. Rev. B* **37,** 785–789

The Rational of Catalytic Activity of Herpes Simplex Virus Thymidine Kinase: A COMBINED BIOCHEMICAL AND QUANTUM CHEMICAL STUDY

Marialore Sulpizi, Pierre Schelling, Gerd Folkers, Paolo Carloni and Leonardo Scapozza

Access the most updated version of this article at doi: 10.1074/jbc.M010223200

Alerts:
- When this article is cited
- When a correction for this article is posted

Click here to choose from all of JBC's e-mail alerts

This article cites 38 references, 7 of which can be accessed free at
http://www.jbc.org/content/276/24/21692.full.html#ref-list-1